THE JOURNAL OF BIOLOGICAL CHEMISTRY VOL. 282, NO. 50, pp. 36321–36329, December 14, 2007

The Caspase-1 Digestome Identifies the Glycolysis Pathway as a Target during Infection and Septic Shock*[S]◆

Received for publication, October 2, 2007, and in revised form, October 23, 2007 Published, JBC Papers in Press, October 24, 2007, DOI 10.1074/jbc.M708182200

Wei Shao[‡], Garabet Yeretssian[§], Karine Doiron[§], Sabah N. Hussain[§], and Maya Saleh[‡§¶1]

From the Departments of [‡]Biochemistry and [§]Medicine, Division of Critical Care, and the [¶]Centre for the Study of Host Resistance, McGill University, Montreal, Quebec H3A 1A1, Canada

Caspase-1 is an essential effector of inflammation, pyroptosis, and septic shock. Few caspase-1 substrates have been identified to date, and these substrates do not account for its wide range of actions. To understand the function of caspase-1, we initiated the systematic identification of its cellular substrates. Using the diagonal gel proteomic approach, we identified 41 proteins that are directly cleaved by caspase-1. Among these were chaperones, cytoskeletal and translation machinery proteins, and proteins involved in immunity. A series of unexpected proteins along the glycolysis pathway were also identified, including aldolase, triose-phosphate isomerase, glyceraldehyde-3-phosphate dehydrogenase, α-enolase, and pyruvate kinase. With the exception of the latter, the identified glycolysis enzymes were specifically cleaved *in vitro* by recombinant caspase-1, but not caspase-3. The enzymatic activity of wild-type glyceraldehyde-3-phosphate dehydrogenase, but not a non-cleavable mutant, was dampened by caspase-1 processing. *In vivo*, stimuli that fully activated caspase-1, including *Salmonella typhimurium* infection and septic shock, caused a pronounced processing of these proteins in the macrophage and diaphragm muscle, respectively. Notably, these stimuli inhibited glycolysis in wild-type cells compared with caspase-1-deficient cells. The systematic characterization of caspase-1 substrates identifies the glycolysis pathway as a caspase-1 target and provides new insights into its function during pyroptosis and septic shock.

Caspases are aspartate-specific cysteine proteases known for their function in regulating programmed cell death and inflammation. Phylogenetically, they are subdivided into the CED3-related enzymes that initiate and execute cell death and the caspase-1-related proteins that process and mature cytokines, *viz.* IL-1β,[2] IL-18, and IL-33. Apoptotic caspases execute cell death through the restricted cleavage of key cellular proteins required to maintain cell viability, resulting in the morphological changes observed during apoptosis, including membrane blebbing, nuclear condensation, and cytoskeletal dismantling (1).

Caspase-1 is essential during inflammation because of its role in the activation of cytokine signaling pathways. With the exception of its cytokine substrates, very little is known regarding the spectrum of cellular proteins it targets upon full activation. Similar to other caspases, caspase-1 is found in cells as an inactive precursor and is activated in response to inflammatory triggers, including pathogen-derived molecules, as well as danger signals released from infected or dying cells (2). Caspase-1 activation is achieved in a macromolecular complex known as the inflammasome through its recruitment to a scaffolding molecule generally via the adaptor ASC (3). Scaffolding molecules that activate caspase-1 within the inflammasome belong to the cytosolic Nod-like family of pathogen recognition receptors and include Nalp1–3, Ipaf, and Naip5 (4). More recently, a distinct caspase-1 activation platform, the ASC pyroptosome, has been characterized (5). It differs from the inflammasome in that it does not contain a Nod-like scaffolding protein but is assembled through the oligomerization of ASC. Although caspase-1 is activated transiently within the Nalp inflammasomes, resulting in controlled inflammation and the restricted processing of cytokine substrates, it is fully activated within the pyroptosome, leading to a distinct form of inflammatory cell death known as pyroptosis (6). Pyroptosis exhibits features common to both apoptosis and necrosis, including nuclear condensation, loss of mitochondrial membrane potential, and membrane swelling (5). It was initially observed in macrophages infected with the intracellular pathogen *Salmonella typhimurium* (7) but was later found to occur in response to infection with other intracellular pathogens (8, 9). Because only a few substrates for caspase-1 have been identified thus far, the mechanism by which caspase-1 kills the cell via pyroptosis remains obscure.

Another instance in which caspase-1 is activated is during septic shock (10, 11). Hyperproduction of cytokines alone does not account for the totality of caspase-1 effects during septic shock. One characteristic of this condition is an impaired ventilatory muscle contractility that causes ventilatory failure and respiratory arrest (12), and caspase-1-deficient mice, but not IL-1β/IL-18 double knock-out mice, are protected from this condition (13).

* This work was supported in part by grants from the Canadian Institutes of Health Research and the Canada Foundation for Innovation. The costs of publication of this article were defrayed in part by the payment of page charges. This article must therefore be hereby marked "*advertisement*" in accordance with 18 U.S.C. Section 1734 solely to indicate this fact.

◆ This article was selected as a Paper of the Week.

[S] The on-line version of this article (available at http://www.jbc.org) contains supplemental Fig. 1 and Table 1.

[1] Canadian Institutes of Health Research New Investigator. To whom correspondence should be addressed: McGill University Health Centre, Rm. M11.41, 687 Pine Ave. W., Montreal, Quebec H3A 1A1, Canada. Tel.: 514-934-1934 (ext. 34416); Fax: 514-843-1686; E-mail: maya.saleh@mcgill.ca.

[2] The abbreviations used are: IL, interleukin; TIM, triose-phosphate isomerase; GAPDH, glyceraldehyde-3-phosphate dehydrogenase; CHAPS, 3-[(3-cholamidopropyl)dimethylammonio]-1-propanesulfonic acid; LPS, lipopolysaccharide; BisTris, 2-[bis(2-hydroxyethyl)amino]-2-(hydroxymethyl)propane-1,3-diol; TBS, Tris-buffered saline; MALDI-TOF, matrix-assisted laser desorption ionization time-of-flight.

To understand the role of caspase-1 in pyroptosis and septic shock, we sought to identify its cellular substrates. Here, we used the diagonal gel proteomic approach and identified multiple caspase-1 direct targets. These included structural proteins, chaperones, translation machinery proteins, and proteins involved in immunity. A series of unexpected proteins along the glycolysis pathway were also identified as caspase-1 substrates, including aldolase, TIM, GAPDH, enolase, and pyruvate kinase. Here, we show that *Salmonella* infection, which fully activates caspase-1 and induces pyroptosis (7), caused a pronounced degradation of these glycolysis enzymes and lowered the glycolytic rate of wild-type macrophages, but not caspase-1-deficient cells. Similarly, we show that the glycolysis enzymes were processed in the diaphragm muscle of wild-type septic mice. Detailed analysis of the caspase-1 substrates is likely to shed light on caspase-1 function in pyroptotic cell death and septic shock.

EXPERIMENTAL PROCEDURES

Antibodies and Reagents—Anti-α-enolase (1:2000 dilution in muscle and 1:1000 dilution in monocytes; catalog no. sc-7455), anti-aldolase (1:2000 dilution in muscle and 1:1000 dilution in monocytes; catalog no. sc-12059), anti-TIM (1:1000 dilution; catalog no. sc-22031), and anti-caspase-1 p10 subunit (1:500 dilution in muscle and 1:1000 dilution in monocytes; catalog no. sc-514) antibodies were purchased from Santa Cruz Biotechnology, Inc. Anti-GAPDH antibody (1:1000 dilution; Ab9485) was obtained from Abcam. Anti-IL-1β antibody (1:1000 dilution; catalog no. 2022) was purchased from Cell Signaling Technology. Human recombinant caspase-1 was from Merck. TRIzol RNA extraction reagent, oligo(dT)$_{12-18}$ primers, random hexamers, and Moloney murine leukemia virus reverse transcriptase were from Invitrogen. RNase inhibitor and an *in vitro* transcription/translation kit were from Promega Corp. The QuikChange site-directed mutagenesis kit was from Stratagene.

Diagonal Gel—18 × 10^6 THP-1 cells or human peripheral blood mononuclear cells were lysed in 200 μl of Laemmli SDS loading buffer (50 mM Tris (pH 6.8), 2% SDS, 0.1% bromphenol blue, 10% glycerol, and 2.5% β-mercaptoethanol) and sonicated three times for 15 s each (with the sonicator speed adjusted to prevent foaming). 400 μg of protein was resolved by 10% SDS-PAGE (first dimension). After migration, the lane containing the protein was excised and soaked in 40% ethanol and 10% acetic acid for 10 min, in ethanol 30% for 10 min, and then in ultrapure water twice for 10 min each. The lane was air-dried until the gel started to curl; soaked in CHEG buffer (0.1% CHAPS, 50 mM HEPES-KOH (pH 7.2), 2 mM EDTA, and 10% glycerol with 5 mM dithiothreitol freshly added) with or without 50 μg of recombinant caspase-1 or caspase-3 (Merck); and incubated overnight at 37 °C in a sealed bag. The lane was washed with water to remove the excess protease and then incubated in Laemmli SDS loading buffer for 10 min in a 95 °C water bath in a conical tube. After cooling, the lane was loaded onto a second dimension 10% SDS-polyacrylamide gel and resolved again. After migration, the gel was fixed in 10% acetic acid and 40% ethanol and then silver-stained. Cleaved proteins, which were located under the diagonal, were excised from the gel and identified by mass spectrometry at the McGill University and Génome Québec Innovation Centre by liquid chromatography-mass spectrometry.

RNA Extraction and Reverse Transcription-PCR—Total RNA was isolated from THP-1 cells using TRIzol reagent. Every 1 × 10^6 cells were lysed in 200 μl of TRIzol and extracted with 40 μl of chloroform. cDNAs were created via reverse transcription using oligo(dT) or random hexamers.

Plasmid Preparation and Site-directed Mutagenesis—Enolase, aldolase, TIM, and pyruvate kinase were amplified by PCR from THP-1 cDNA. For the primers used, please see supplemental Table 1. The PCR products were cloned into the pcDNA3.1/neo vector. The plasmids cloned from cDNA were confirmed by sequencing. The GAPDH cDNA was purchased from American Type Culture Collection (catalog no. 57091) and recloned into the pcDNA3.0 vector. Potential cleavage site mutations were introduced by site-directed mutagenesis using the QuikChange site-directed mutagenesis kit following the manufacturer's instructions. The primers for GAPDH(D189A) were 5′-CTGCCACCCAGAAGACTGTGGCTGGCCCCTCCGGGAAACTGTG-3′ (forward) and 5′-CACAGTTTCCCGGAGGGGCCAGCCACAGTCTTCTGGGTGGCAG-3′ (reverse).

Cloning Primers for PCR—cDNA cloning site primers were as follows: GAPDH, 5′-GCGGCTCGAGATGGGGAAGGTGAAGGTCGG-3′ (XhoI, forward) and 5′-GCGGGAATCCTTACTCCTTGGAGGCCATGTGGG-3′ (EcoRI, reverse); α-enolase, 5′-GCGGAAGCTTATGTCTATTCTCAAGATCCATGCC-3′ (HindIII, forward) and 5′-GCGGGCGGCCGCTTACTTGGCCAAGGGG-3′ (NotI, reverse); aldolase, 5′-GGCCAAGCTTATGCCCTACCAATATCCAGC-3′ (HindIII, forward) and 5′-GCGGGCGGCCGCTTAATAGGCGTGGTTAGAGACG-3′ (NotI, reverse); α-enolase, 5′-GCGGAAGCTTCGGACAGTATCTGTGGGTACC-3′ (HindIII, forward) and 5′-GCGGGCGGCCGCCGAGCTGCCTGAGCTGACACG-3′ (NotI, reverse); aldolase, 5′-GCGGAAGCTTGGGGTGCCTCAACCACACTCCG-3′ (HindIII, forward) and 5′-GCGGGCGGCCGCGCCCCGAGGAGGCGGCCTCC-3′ (NotI, reverse); TIM, 5′-GGCGAAGCTTATGGCGCCCTCCAGGAAGTTCTTCG-3′ (HindIII, forward) and 5′-GGCGGCGGCCGCTCATTGTTTGGCATTGATGATGTCC-3′ (NotI, reverse); and pyruvate kinase, 5′-GGCGGCGGCCGCATGTCGAAGCCCCATAGTGAAGCCGGG-3′ (NotI, forward) and 5′-GGCGCTCGAGTCACGGCACAGGAACAACACGCATGG-3′ (XhoI, reverse).

In Vitro Transcription/Translation—[^{35}S]Methionine-labeled substrates were obtained by coupled *in vitro* transcription/translation using the Promega TNT reticulocyte lysate system or the wheat germ lysate system. 0.7 μg of the cDNA constructs was incubated with T7 polymerase, rabbit reticulocyte or wheat germ lysate, amino acid mixture minus methionine, and [^{35}S]methionine for 1.5 h at 30 °C.

Caspase Cleavage Assays—Cleavage of the *in vitro* transcribed and translated ^{35}S-labeled substrates was performed in a 20-μl reaction containing 2 μl of *in vitro* transcribed and translated ^{35}S-labeled substrates by incubation at 37 °C for 4 h in the presence or absence of purified human recombinant caspase-1 (170 ng) in CHEG buffer (with 10 mM dithiothreitol

freshly added). The cleavage reaction was terminated by the addition of Laemmli SDS loading buffer and resolved by SDS-PAGE. The gel was fixed in 10% acetic acid and 40% ethanol for 0.5 h; the signal was then amplified by incubating the gel with NAMP 100V amplifying solution (Amersham Biosciences) for 30 min. The gel was placed on a Whatman paper, dried at 70 °C for 1 h, and exposed at −80 °C, and the signal was viewed by autoradiography.

Salmonella Preparation for Infection—*Salmonella* strain SL1344 was cultured aerobically at 37 °C in LB broth or on LB agar without antibiotics. Bacteria were freshly plated on LB agar. To obtain stationary-phase bacteria for infection of THP-1 cells, LB broth was inoculated with a single colony and grown overnight in 3 ml of LB broth with shaking. The next day, before infection, bacteria were diluted 1:10 in LB broth and grown to $A_{600} = 0.9$ (equivalent to 10^5 bacteria/μl) at 50 rpm/min (~3.5 h), and then bacteria were harvested by centrifugation at 10,000 rpm for 1 min, washed once with an equal amount of phosphate-buffered saline and once with culture medium (without antibiotics), and incubated for 20 min at 37 °C in cell culture medium (without antibiotics) in a tissue culture incubator in a conical tube with the cap loose. The bacteria were used immediately for infection of cells.

Cell Culture and Infection—THP-1 cells were maintained at a density of ~1×10^6 cells/ml. 1 day prior to infection, cells (5 ml at 1×10^6 cells/ml) were harvested, washed, and resuspended in fresh medium without antibiotics in a 10-cm plate. THP-1 cells were incubated overnight with phorbol 12-myristate 13-acetate (20 ng/ml) to differentiate the cells into adherent macrophage-like cells. The next day, the medium and non-adherent cells were removed and replaced with fresh medium without antibiotics. The cells were then primed overnight with 50 ng/ml crude *Escherichia coli* LPS (serotype 0111:B4 L4391; Sigma). The next day, cells were infected with *Salmonella* at a multiplicity of infection of 1:1, 5:1, or 10:1 bacteria/THP-1 cells. Culture plates were centrifuged at 500 × *g* for 10 min and incubated at 37 °C for 30 min to allow phagocytosis to occur. The medium was then replaced with fresh medium without antibiotics and incubated for an additional 4–16 h.

Preparation of Peritoneal Macrophages—Wild-type (C57BL/6) and caspase-1 knock-out (back-crossed onto the C57BL/6 background) mice were injected intraperitoneally with 2 ml of 3% thioglycolate, and peritoneal macrophages were collected after 96 h. Briefly, mice were intraperitoneally injected with 5 ml of RPMI 1640 medium using a 26.5-gauge needle, and peritoneal macrophages were taken out with a 5-ml syringe and an 18-gauge needle. The cell suspension was passed through a 100-μm filter, spun, and resuspended in fresh medium. 10^5 cells/well were plated in a 96-well plate.

Mouse Model of LPS-induced Septic Shock—C57BL/6 mice (8–12 weeks old) were injected intraperitoneally with 20 mg/kg LPS from *E. coli* (serotype 055:B5; Sigma). Control mice were injected intraperitoneally with saline. The mice were killed 12 or 24 h post-injection by injection of 60 mg/kg pentobarbital. The diaphragm muscle (100 mg) was homogenized in 1 ml of buffer containing 20 mM HEPES (pH 7.4), 0.2 mM phenylmethylsulfonyl fluoride, 1 μM leupeptin, 1 μM pepstatin A, 0.4 mM EDTA, 0.2 mM sodium orthovanadate, and 30 mM sodium fluoride and then centrifuged at 14,000 × *g* for 20 min, and the supernatant was collected for Western blotting.

Lactate Measurement—Peritoneal macrophages from wild-type or caspase-1 knock-out mice were plated in 96-well plates at a density of 1×10^5 cells/well. The cells were primed overnight with LPS (50 ng/ml) and then infected with *Salmonella* at a multiplicity of infection of 10:1 bacteria/peritoneal macrophages. After 4 h of infection, the culture medium was collected for lactate measurement using a kit from Trinity Biotech (catalog no. 735-10) following the manufacturer's instructions. Briefly, 10 μl of cell culture medium was incubated with 1 ml of lactate reagent at room temperature for 10 min, and then the absorbance was read at 540 nm. The lactate concentration was calculated using an equation derived from a standard absorbance.

GAPDH Assay—The assay mixture (1 ml) contained 10 mM sodium phosphate buffer (pH 7.8), 1 mM EDTA, 1 mM glyceraldehyde 3-phosphate (catalog no. G-5251, Sigma), 0.5 mM NAD^+, and GAPDH from THP-1 cell lysates in CHEG buffer (80 μg of total protein) or *in vitro* transcribed and translated GAPDH and GAPDH(D189A) (10 μl). The reaction was initiated by the addition of GAPDH to the assay mixture, and the activity was monitored by NAD reduction at 340 nm. Absorbance was recorded every 10 s during 5 min.

Sample Preparation for GAPDH Assay—For the assay using GAPDH from cell lysates, THP-1 cells were lysed in CHEG buffer, and 80 μg total proteins was diluted in 100 μl of CHEG buffer and incubated with or without 170 ng of caspase-1 at 37 °C for 3 h. For the assay using *in vitro* transcribed and translated GAPDH or its mutant D189A, *in vitro* transcribed and translated products (10 μl) were diluted in a total of 20 μl of CHEG buffer and then incubated with or without caspase-1 for 3 h.

Western Blotting—For Western blotting, 1.2×10^6 cells were lysed in 100 μl of 1× SDS-PAGE buffer, sonicated three times for 10 s each, and then spun down at 13,000 rpm for 15 min. 40 μl was loaded onto a 4–12% Criterion XT precast BisTris/SDS-polyacrylamide gel (Bio-Rad), migrated at 125 V for 1.5 h, and transferred onto nitrocellulose membrane at 50 V for 1 h. The membrane was then blocked in 5% milk in TBS containing 0.1% Tween for 1 h at room temperature. The primary antibodies were diluted as described above in 5% milk in TBS containing 0.1% Tween and incubated overnight with the membrane with shaking at 4 °C. The blot was washed three times for 10 min each with TBS containing 0.1% Tween at room temperature. The secondary antibodies were diluted as described above in 5% milk in TBS containing 0.1% Tween and incubated with the membrane for 1 h at room temperature. The blot was washed three times for 5 min each with TBS containing 0.3% Tween and then three times for 5 min each with TBS containing 0.1% Tween. The signal was developed by incubating the blot with SuperSignal West Femto maximum sensitivity substrate reagent (catalog no. 34095, Pierce) for 5 min at room temperature.

RESULTS

The Caspase-1 Digestome—To identify caspase-1 substrates, we used the diagonal gel proteomic approach (14). In this method, cellular proteins are separated on a first dimension

denaturing SDS-polyacrylamide gel lane, which after migration is washed to remove residual SDS, dehydrated, and then rehydrated in a caspase activation buffer containing the caspase of choice. Following the in-gel processing of the caspase substrates, the gel lane is loaded horizontally on a second dimension SDS-polyacrylamide gel, resulting in the migration of the majority of cellular proteins along a diagonal line and of the cleaved proteins under the diagonal (Fig. 1, *A* and *B*). The cleavage products were identified by mass spectrometry. To validate the method, we initially screened for caspase-3 targets and identified multiple caspase-3 known substrates along with novel substrates (Table 1) (data not shown). For the caspase-1 screen, we chose to work with cell lysates from LPS-stimulated THP-1 macrophages as a source of cellular proteins on the diagonal gel. To control for the caspase-1 digestion, we performed a Western blot on the caspase-1 diagonal gel and detected the drop of mature IL-1β under the diagonal at 17 kDa as expected (Fig. 1*C*). Spots that dropped under the diagonal on the caspase-1 gel were excised and processed for mass spectrometry. After eliminating hits with <10% peptide coverage of the sequence of the cleaved product, we obtained 41 proteins that were processed by caspase-1. These included proteins involved in different processes essential for cell survival, such as translation, cytoskeletal architecture and function, signaling, and energy metabolism (Fig. 1*D*). These processes were also targeted by caspase-3 in the diagonal gel screen and are targeted by executioner caspases *in vivo* during apoptosis.

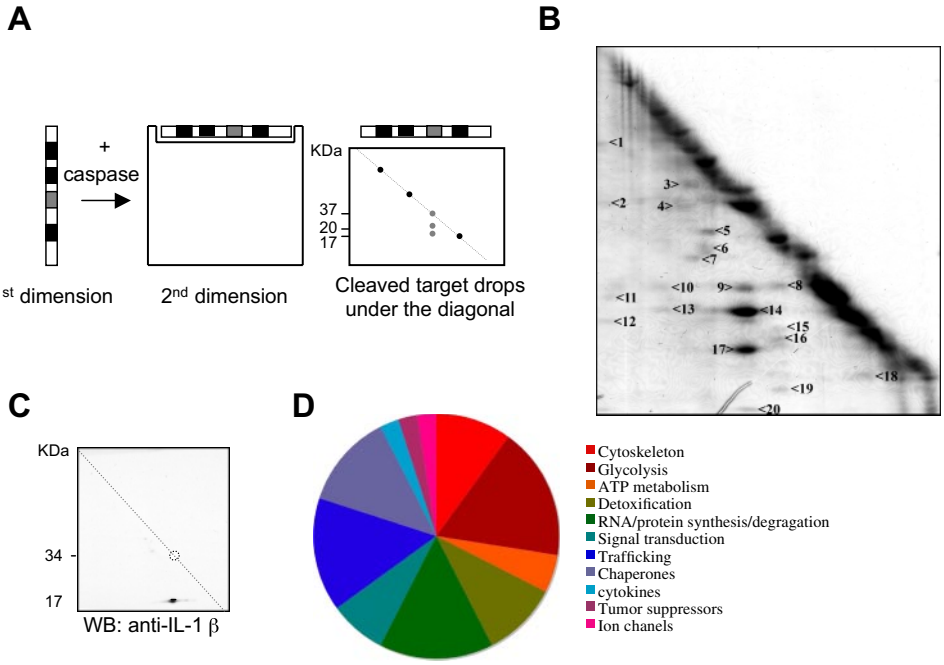

FIGURE 1. **Caspase-1 substrates identified by the diagonal gel approach.** *A*, a schematic representation of the diagonal gel method. Whole cell lysates are separated on a first dimension SDS-polyacrylamide gel; the gel lane is excised and dehydrated and then rehydrated in the presence of the caspase of choice. The processed gel lane is next migrated on a second dimension SDS-polyacrylamide gel. The majority of proteins migrate along the diagonal line, whereas fragments of the substrates cleaved by the caspase drop under the diagonal and are then processed for identification by MALDI-TOF mass spectrometry. *B*, an example of the diagonal gels run in this study. Whole cell extracts were subjected to SDS-PAGE and digested with the recombinant caspase. The second dimension gel was silver-stained. The marked spots were excised and processed for MALDI-TOF analysis. *C*, validation of the caspase-1 diagonal gel approach by Western blotting (*WB*) with an antibody against the known caspase-1 substrate pro-IL-1β. Whole cell lysates were prepared from LPS-stimulated THP-1 cells. *D*, a pie chart representing the cellular pathways targeted by caspase-1.

TABLE 1

List of the known caspase substrates and glycolysis enzyme substrates that were identified in the caspase-1 or caspase-3 diagonal gel experiments by liquid chromatography-mass spectrometry

References are for the original reports identifying the listed substrates. For a complete list of caspase-1 substrates identified in this study, see supplemental Table 1. hnRNP, heterogeneous nuclear ribonucleoprotein; snRNP, small nuclear ribonucleoprotein.

Protein	GenBank™ accession no.	Function	Caspase-1	Caspase-3	Known caspase substrate	Ref.
Cellular myosin heavy chain	gi 553596	Cytoskeletal protein		×	×	30
F-actin capping protein subunit a	gi 5453597	Cytoskeletal protein	×	×	×	33
Filamin-1	gi 4503745	Cytoskeletal protein		×	×	34
Gelsolin isoform a	gi 4504165	Cytoskeletal protein		×	×	35
Gelsolin isoform b	gi 38044288	Cytoskeletal protein		×	×	35
Vimentin	gi 37852	Cytoskeletal protein		×	×	36
α-Actin	gi 178027	Cytoskeletal protein		×	×	37
α-Tubulin	gi 15010550	Cytoskeletal protein		×	×	30
γ-Actin	gi 178045	Cytoskeletal protein	×	×	×	37
HSP90	gi 306891	Chaperone	×	×	×	38
hnRNP A1	gi 133254	Spliceosome		×	×	39
U2 snRNP A′	gi 18605961	Spliceosome				31
Nascent polypeptide-associated complex	gi 5031931	Translation	×	×	×	40
Polypyrimidine tract-binding protein-1	gi 4506243	Spliceosome		×	×	31
Caspase-1	gi 2914146	Maturation of cytokines and pyroptosis	×		×	
Glycolysis						
Aldolase A	gi 28614	Glycolysis	×			
TIM	gi 136066	Glycolysis	×			
GAPDH	gi 31645	Glycolysis	×			
α-Enolase	gi 4503571	Glycolysis	×			
Pyruvate kinase	gi 35505	Glycolysis	×	×		

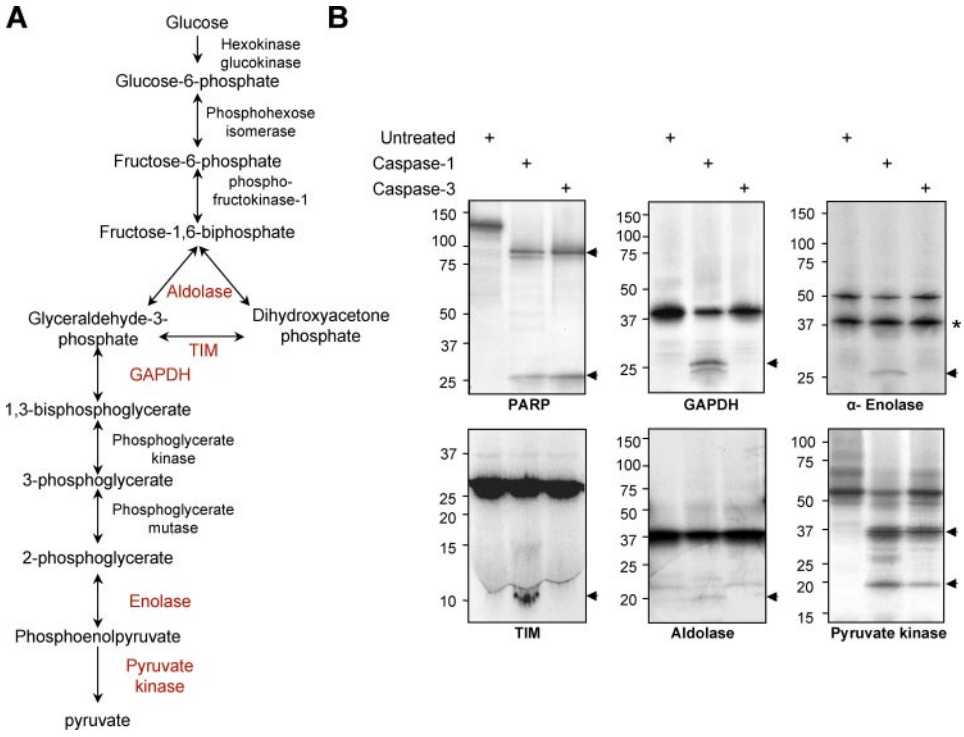

FIGURE 2. **Caspase-1 targets the glycolysis pathway.** *A*, a representation of the glycolysis pathway and the glycolysis enzymes targeted by caspase-1 (shown in *red*). Glucose is converted to pyruvate via the action of the glycolysis enzymes. Five glycolysis enzymes were identified on the caspase-1 diagonal gel. *B*, cleavage of *in vitro* transcribed and translated glycolysis enzymes by caspase-1 and caspase-3. *In vitro* transcribed and translated [^{35}S]methionine-labeled poly(ADP-ribose) polymerase (*PARP*), GAPDH, TIM, α-enolase, aldolase, and pyruvate kinase were incubated with or without recombinant caspase-1 (170 ng) or caspase-3 (290 ng) for 4 h at 37 °C. *Arrowheads* indicate cleavage products. The *asterisk* indicates an internal translation product of enolase.

Despite acting on common cellular pathways, caspase-1 and caspase-3 did not cleave the same proteins along these pathways. 30% of the caspase-1 substrates were also processed by caspase-3, whereas the remaining 70% were specific to caspase-1.

Caspase-1 Targets the Glycolysis Pathway—Multiple proteins involved in energy metabolism along the glycolysis pathway were identified in the caspase-1 diagonal gel screen (Fig. 2*A* and Table 1). To validate this result, we first performed *in vitro* caspase cleavage assays. Although both caspase-1 and caspase-3 processed an *in vitro* transcribed and translated [^{35}S]methionine-labeled form of the classical caspase target poly(ADP-ribose) polymerase (15), only caspase-1, but not caspase-3, cleaved the glycolysis enzymes aldolase, TIM, GAPDH, and enolase (Fig. 2*B*). On the other hand, pyruvate kinase was cleaved by both caspases (Fig. 2*B*). Because the cleavage of GAPDH by caspase-1 was more efficient than that of the other glycolysis enzymes *in vitro*, we further characterized this cleavage event. The addition of increasing amounts of caspase-1 led to enhanced GAPDH processing in a dose-dependent manner (Fig. 3*A*). In comparison with the full processing of pro-IL-1β by caspase-1 that required 1 ng of our caspase-1 preparation, maximum cleavage of the GAPDH proform required 50 ng of the enzyme (Fig. 3*A*), suggesting that *in vivo*, GAPDH processing would occur under conditions in which caspase-1 is fully activated, leading to pyroptotic cell death, rather than in response to stimuli that activate caspase-1, transiently leading to cytokine maturation. Caspase processing could lead to either a gain- or loss-of-function consequence for the substrate. To examine the effect of caspase-1 on GAPDH function, we performed GAPDH enzymatic activity assays *in vitro* in the presence or absence of caspase-1. Our results indicated that incubation of cell lysates with caspase-1 diminished GAPDH activity by up to 70% compared with the activity measured in the absence of caspase-1 (Fig. 3*B*), suggesting a loss-of-function effect of caspase-1 on GAPDH. We next sought to identify the caspase-1 cleavage site in GAPDH. On the basis of the size of the cleavage product, we mapped four potential caspase cleavage sites and mutated their corresponding aspartic acid residues to alanine (Fig. 3*C*). We then performed *in vitro* caspase cleavage assays and identified the sequence KTVD^{189}↓G as the caspase-1 cleavage site in GAPDH. The mutation D189A abrogated the processing of GAPDH by caspase-1 (Fig. 3*D*). Alignment of protein sequences from different species revealed that the caspase-1 cleavage site in GAPDH and the sequence flanking it have been highly conserved throughout evolution (Fig. 3*E*). To address the significance of the caspase-1 cleavage, we compared the enzymatic activity of wild-type GAPDH with that of the D189A mutant, which is resistant to caspase-1 cleavage, in the absence or presence of active caspase-1. GAPDH enzymatic activity assays indicated that although the activity of *in vitro* transcribed and translated wild-type GAPDH was reduced by 50% in the presence of active caspase-1, that of the non-cleavable mutant was mostly retained, diminishing by only 10% compared with the activity measured in the absence of caspase-1 (Fig. 3*F*).

Caspase-1 Activation during Salmonella Infection Leads to the Processing of the Glycolysis Enzymes and Reduction of the Cellular Glycolytic Rate—To confirm that the glycolysis enzymes identified in the caspase-1 diagonal gel screen are *bona fide* caspase-1 substrates, the next step was to examine whether they are processed *in vivo* under conditions that lead to caspase-1 activation. We chose to address this question in macrophages because they are known to depend on glycolysis for energetic demands (16) and to produce most of their ATP through glycolysis (17, 18). Although glycolytic inhibitors reduce both cellular ATP and effector functions of macrophages and neutrophils, inhibitors of mitochondrial respiration have little effect on these processes (19, 20). In addition, an increase in glycolysis occurs in activated macrophages and is required for effector functions, including adhesion, extravasa-

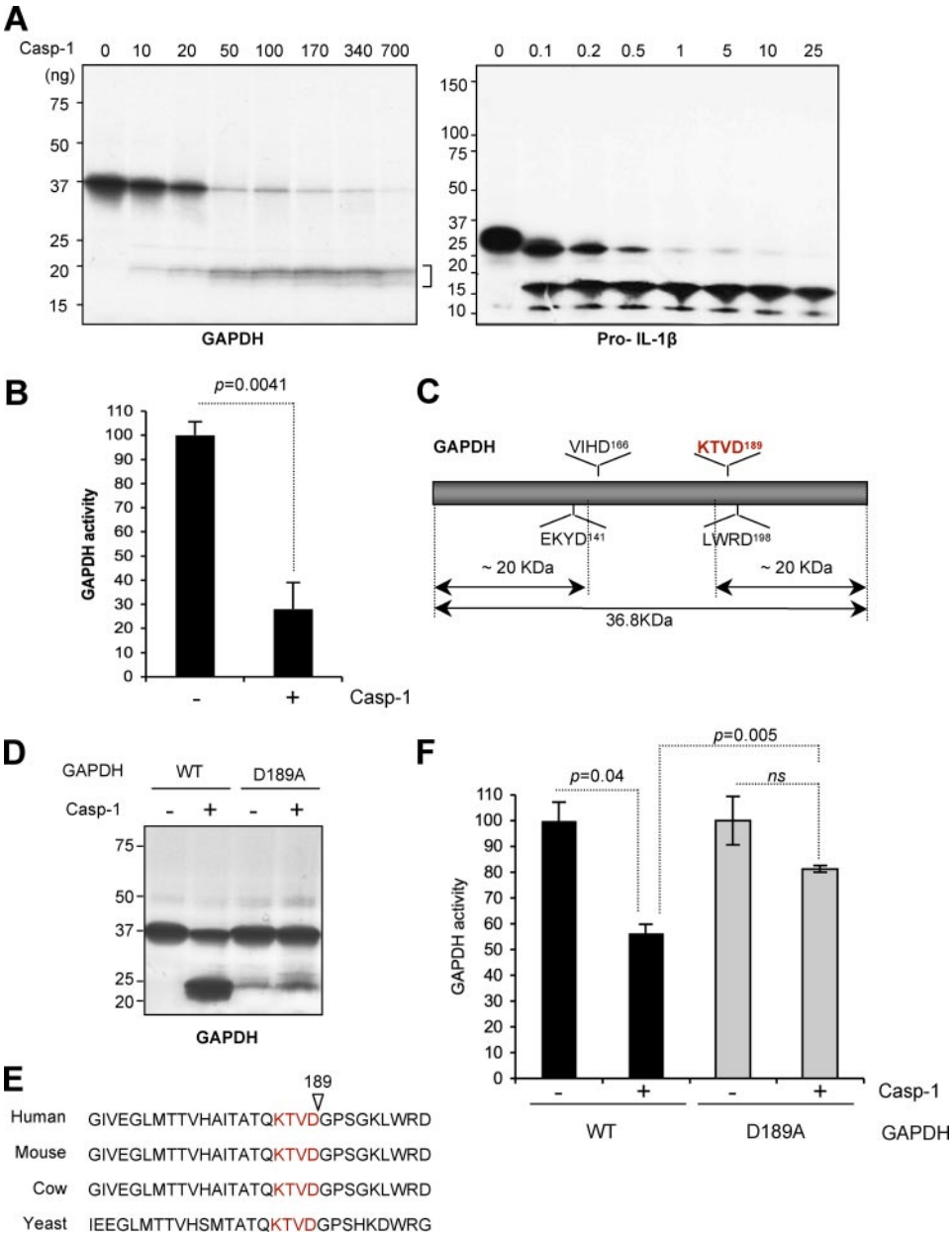

FIGURE 3. **Characterization of GAPDH cleavage by caspase-1.** *A*, increasing the amount of caspase-1 (*Casp-1*) resulted in enhanced processing of GAPDH. *B*, GAPDH activity was affected by the caspase-1 cleavage. THP-1 lysates were incubated with or without caspase-1 (170 ng) for 3 h. GAPDH activity was measured by spectroscopy as described under "Experimental Procedures." *C*, shown are the results from the analysis of the potential cleavage sites in GAPDH that could result in a 25-kDa cleavage product. *D*, GAPDH(D189A) is resistant to caspase-1 cleavage. *E*, shown is the alignment of the region containing the caspase-1 cleavage site in GAPDH from different species. *F*, the activity of the non-cleavable mutant GAPDH(D189A) is retained in the presence of caspase-1. Wild-type (*WT*) GAPDH and GAPDH(D189A) were synthesized by coupled *in vitro* transcription/translation using wheat germ lysates and were used in the GAPDH enzymatic assay as described under "Experimental Procedures." *ns*, not significant.

tion, motility, and invasion (21–23). To activate caspase-1 *in vivo*, we treated differentiated THP-1 macrophages with LPS and ATP or with LPS and nigericin, stimuli that cause potassium efflux, resulting in caspase-1 activation within the Nalp3 inflammasome (24). On the other hand, we infected THP-1 cells with the intracellular pathogen *S. typhimurium*, which activates caspase-1 within the Ipaf inflammasome (25, 26). In both instances, pro-IL-1β was processed into its 17-kDa mature form by caspase-1 (Fig. 4*A*, *upper panels*). When cells were treated with LPS and ATP or with LPS and nigericin, we did not detect caspase-1-specific cleavage products. We observed 30- and 17-kDa bands, but these were also found when cells were treated with LPS only, a condition under which caspase-1 was not activated as evidenced by the lack of IL-1β processing (Fig. 4*A*). On the other hand, aldolase was fully processed and degraded during *Salmonella* infection in a multiplicity of infection-dependent manner (Fig. 4*A*, *lower left panel*). Similarly, enolase was cleaved and degraded during *Salmonella* infection (supplemental Fig. 1). We assume that the slightly faster migrating band on the enolase Western blot corresponds to bacterial enolase, as it was also detected in the bacterial lysate (*BL lane*). We were unable to assess the processing of GAPDH in *Salmonella*-infected cells because our anti-GAPDH antibodies reacted with bacterial GAPDH upon Western blotting (data not shown). To investigate whether the *Salmonella*-induced degradation of the glycolysis enzymes was mediated by caspase-1, we examined aldolase processing in *Salmonella*-infected peritoneal macrophages derived from wild-type or caspase-1-deficient mice (10). We observed that aldolase was degraded in wild-type macrophages infected with *Salmonella*, but not in infected caspase-1-deficient macrophages (Fig. 4*B*), confirming the role of caspase-1 in aldolase processing *in vivo*. We next assessed whether the processing of the glycolysis enzymes had an impact on the overall glycolytic rate of the cell. One marker of enhanced glycolytic function and inflammatory activation of macrophages is the increase in lactate production (27). We measured lactate levels in wild-type and caspase-1-deficient cells treated with ATP or nigericin or infected with *Salmonella*. Our results indicated that activation of caspase-1 resulted in marked reduction of glycolysis, as lactate levels were consistently higher in caspase-$1^{-/-}$ macrophages compared with caspase-$1^{+/+}$ cells in response to *Salmonella* infection (Fig. 4*C*).

The Caspase-1 Substrates in the Glycolysis Pathway Are Cleaved in the Diaphragm Muscle of Mice in Septic Shock—Our results indicate that caspase-1 targets the glycolysis pathway both *in vitro* and *in vivo*, resulting in marked reduction of the

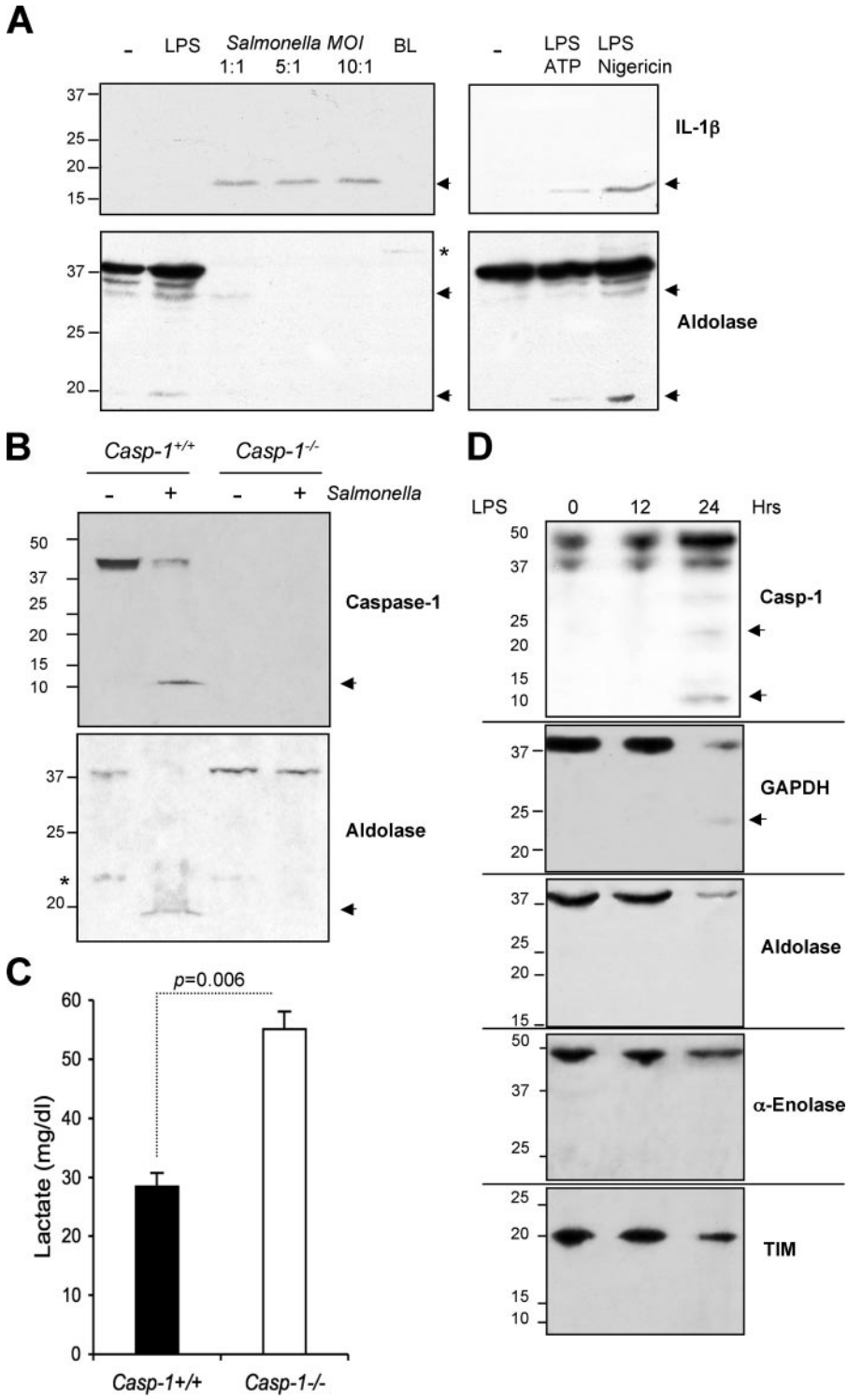

FIGURE 4. **Processing of the glycolysis enzymes *in vivo*.** *A*: *left panels*, macrophages were primed overnight with LPS and then infected with *Salmonella* at increasing multiplicities of infection (*MOI*) of 1:1, 5:1, and 10:1 bacteria/THP-1 cells. *Right panels*, macrophages were treated overnight with LPS, pulsed with ATP (5 mM) or nigericin (20 μM) for 20 min, and then incubated in fresh medium for an additional 3 h. Western blotting was performed using antibodies against mature IL-1β and aldolase. *Arrowheads* indicate cleavage products. The *asterisk* indicates a cross-reacting protein in the bacterial lysates. *BL lane*, bacterial lysate. *B*: aldolase was processed in response to *Salmonella* infection in peritoneal macrophages derived from wild-type mice (*Casp-1*$^{+/+}$), but not in caspase-1-deficient macrophages (*Casp-1*$^{-/-}$). *C*: caspase-1 activation dampened lactate production. Peritoneal macrophages derived from either wild-type or caspase-1-deficient mice were infected with *Salmonella*. Lactate production was measured as described under "Experimental Procedures." *D*: shown is the processing of the glycolysis enzymes in the diaphragm muscle of mice undergoing septic shock. Mice were injected intraperitoneally with 20 mg/kg LPS to induce septic shock. Mice were killed at 12 or 24 h post-injection. The diaphragm muscle was excised, and proteins were extracted and analyzed by Western blotting. *Arrows* indicate cleavage products.

cellular glycolytic rate. It has been shown previously that mice undergoing septic shock have defects in diaphragm muscle contractility, which are associated with a decrease in glycolytic rate (12). Caspase-1-deficient mice are resistant to septic shock-induced mortality (10, 11), whereas IL-1β/IL-18 double knock-out mice are not (13). This suggests that the effects of caspase-1 in septic shock are not solely mediated by its role in processing these two cytokines. Activated caspase-1 must be targeting other substrates that lead to organismal failure and lethality. We investigated whether the glycolysis substrates were processed by caspase-1 in the diaphragm muscle of mice undergoing endotoxic shock. Using Western blot analysis, we detected the activation of caspase-1 in the diaphragm muscle 24 h following LPS injection in wild-type mice. Concomitantly, the levels of GAPDH, aldolase, enolase, and TIM were significantly lower in the septic shock muscle than in the control muscle (Fig. 4*D*). Additionally, GAPDH was processed into a 25-kDa cleavage product corresponding to the caspase-1 cleavage product observed in the *in vitro* cleavage assay. Our results thus suggest that caspase-1 targets the glycolysis enzymes in the diaphragm muscle of mice in septic shock.

DISCUSSION

In this study, we identified 41 cellular proteins that were processed by caspase-1 *in vitro* using the diagonal gel proteomic approach. Among these were five glycolysis enzymes, *viz.* aldolase, TIM, GAPDH, α-enolase, and pyruvate kinase. We validated that these substrates were processed by caspase-1 in *in vitro* cleavage assays. We mapped the caspase-1 cleavage site in GAPDH and showed that although wild-type GAPDH lost its enzymatic activity following incubation with caspase-1, a non-cleavable mutant was resistant to processing and retained its activity in the presence of caspase-1. Additionally, we demonstrated the processing of these substrates *in vivo*

under conditions in which caspase-1 was fully active, such as in macrophage infection with *Salmonella* and in a mouse model of endotoxic shock. These conditions are associated with pyroptosis, a specialized form of cell death mediated by caspase-1. Our results showing an overlap between caspase-1 and caspase-3 substrates are in agreement with the observation that pyroptosis shares certain morphological features with apoptosis (5). Our findings also suggest that caspase-1 acts as an initiator as well as an executioner caspase during pyroptosis, cleaving directly cellular substrates. Because glycolysis is essential for macrophage survival and activation (16), the cleavage of the glycolysis substrates, which results in reduction of cellular glycolysis, is therefore predicted to be an essential step toward cell death. Multiple proteins are targeted by caspase-1 in this pathway. Therefore, it was not possible to substitute them simultaneously with non-cleavable mutants to study whether they would sustain glycolysis and delay cell death. Our results in the diaphragm muscle similarly show that these glycolysis enzymes are cleaved by caspase-1. We propose that the processing of these proteins might contribute to the loss of muscle contractility that occurs in septic shock.

It is interesting to note that during *Salmonella* infection, aldolase was fully degraded and that the degradation did not occur in caspase-1-deficient cells (Fig. 4*B*). It is possible that the caspase-1 cleavage products were targeted for degradation. This has been shown recently to occur for other caspase-cleaved substrates (28) and might represent a mechanism by which the cell clears altered proteins.

In addition to the diagonal gel method described here and in Ref. 14, multiple approaches have been used to identify caspase substrates. These included, among others, the addition of an active recombinant caspase to an *in vitro* transcribed and translated cDNA library (29), comparative two-dimensional gels that separate cell lysates derived from normal or dying cells (30), and chemical modification of proteins generated in cells undergoing apoptosis to reveal endogenous sites (31). Digestion of proteins synthesized by coupled transcription/translation has some advantages in that the whole proteome could be synthesized rapidly and screened systematically for caspase substrates. However, one disadvantage is that many proteins would lack post-translational modifications and might not be folded properly. Two-dimensional gels and the chemical modification of protein methods are advantageous in that caspases are activated at physiological levels. However, other proteases might also be activated, leading to protein processing. Indeed, this was observed in the latter approach, where nonspecific *in vivo* protein processing occurred during Fas-induced apoptosis (31). The advantage of the diagonal gel approach is the use of cell lysates instead of *in vitro* transcribed and translated proteins and of in-gel digestion, which results in direct processing of caspase targets. Because the proteomics technology used in the various screening approaches detects the most abundant proteins in the proteome, we expect more caspase-1 substrates to exist in the cell. These substrates might be masked as well by other factors, such as the type of cells and stimuli used, the charge and molecular weights of the substrates, cellular compartmentalization, and the rate at which these substrates are processed.

In summary, using the diagonal gel proteomic approach, we uncovered 41 novel caspase-1 substrates. We report that the glycolysis pathway is specifically targeted by caspase-1 under conditions in which it is fully active, leading to pyroptosis such as in macrophages infected with *Salmonella* as well as in the diaphragm muscle during endotoxic shock. It is interesting to note that GAPDH was found recently to be a survival protein required for the autophagy of depolarized mitochondria during caspase-independent cell death (32). It is therefore tempting to hypothesize that caspase-1 targets GAPDH not only to abrogate glycolysis but also to inhibit its function in autophagy, which is associated with cell survival. In conclusion, this study broadens our view of the cellular proteins cleaved by caspase-1, beyond its cytokine substrates, and starts to address the mechanism by which caspase-1 executes pyroptosis.

REFERENCES

1. Nicholson, D. W. (1999) *Cell Death Differ.* **6,** 1028–1042
2. Scott, A. M., and Saleh, M. (2007) *Cell Death Differ.* **14,** 23–31
3. Mariathasan, S., and Monack, D. M. (2007) *Nat. Rev. Immunol.* **7,** 31–40
4. Tschopp, J., Martinon, F., and Burns, K. (2003) *Nat. Rev. Mol. Cell Biol.* **4,** 95–104
5. Fernandes-Alnemri, T., Wu, J., Yu, J. W., Datta, P., Miller, B., Jankowski, W., Rosenberg, S., Zhang, J., and Alnemri, E. S. (2007) *Cell Death Differ.* **14,** 1590–1604
6. Saleh, M., and Green, D. R. (2007) *Cell Death Differ.* **14,** 1559–1560
7. Monack, D. M., Navarre, W. W., and Falkow, S. (2001) *Microbes Infect.* **3,** 1201–1212
8. Fink, S. L., and Cookson, B. T. (2005) *Infect. Immun.* **73,** 1907–1916
9. Swanson, M. S., and Molofsky, A. B. (2005) *Autophagy* **1,** 174–176
10. Kuida, K., Lippke, J. A., Ku, G., Harding, M. W., Livingston, D. J., Su, M. S., and Flavell, R. A. (1995) *Science* **267,** 2000–2003
11. Li, P., Allen, H., Banerjee, S., Franklin, S., Herzog, L., Johnston, C., McDowell, J., Paskind, M., Rodman, L., Salfeld, J., Towne, E., Tracey, D., Wardwell, S., Wei, F.-Y., Wong, W., Kamen, R., and Seshadri, T. (1995) *Cell* **80,** 401–411
12. Hussain, S. N. (1998) *Mol. Cell. Biochem.* **179,** 125–134
13. Sarkar, A., Hall, M. W., Exline, M., Hart, J., Knatz, N., Gatson, N. T., and Wewers, M. D. (2006) *Am. J. Respir. Crit. Care Med.* **174,** 1003–1010
14. Ricci, J. E., Munoz-Pinedo, C., Fitzgerald, P., Bailly-Maitre, B., Perkins, G. A., Yadava, N., Scheffler, I. E., Ellisman, M. H., and Green, D. R. (2004) *Cell* **117,** 773–786
15. Gu, Y., Sarnecki, C., Aldape, R. A., Livingston, D. J., and Su, M. S. (1995) *J. Biol. Chem.* **270,** 18715–18718
16. Cramer, T., Yamanishi, Y., Clausen, B. E., Forster, I., Pawlinski, R., Mackman, N., Haase, V. H., Jaenisch, R., Corr, M., Nizet, V., Firestein, G. S., Gerber, H. P., Ferrara, N., and Johnson, R. S. (2003) *Cell* **112,** 645–657
17. Kawaguchi, T., Veech, R. L., and Uyeda, K. (2001) *J. Biol. Chem.* **276,** 28554–28561
18. Lewis, J. S., Lee, J. A., Underwood, J. C., Harris, A. L., and Lewis, C. E. (1999) *J. Leukocyte Biol.* **66,** 889–900
19. Borregaard, N., and Herlin, T. (1982) *J. Clin. Investig.* **70,** 550–557
20. Kellett, D. N. (1966) *J. Pharm. Pharmacol.* **18,** 199–200
21. Simchowitz, L., Mehta, J., and Spilberg, I. (1979) *Arthritis Rheum.* **22,** 755–763
22. Weisdorf, D. J., Craddock, P. R., and Jacob, H. S. (1982) *Blood* **60,** 888–893
23. Weisdorf, D. J., Craddock, P. R., and Jacob, H. S. (1982) *Inflammation* **6,** 245–256
24. Mariathasan, S., Weiss, D. S., Newton, K., McBride, J., O'Rourke, K., Roose-Girma, M., Lee, W. P., Weinrauch, Y., Monack, D. M., and Dixit, V. M. (2006) *Nature* **440,** 228–232
25. Miao, E. A., Alpuche-Aranda, C. M., Dors, M., Clark, A. E., Bader, M. W., Miller, S. I., and Aderem, A. (2006) *Nat. Immunol.* **7,** 569–575
26. Franchi, L., Amer, A., Body-Malapel, M., Kanneganti, T. D., Ozoren, N., Jagirdar, R., Inohara, N., Vandenabeele, P., Bertin, J., Coyle, A., Grant, E. P., and Nunez, G. (2006) *Nat. Immunol.* **7,** 576–582

27. Haji-Michael, P. G., Ladriere, L., Sener, A., Vincent, J. L., and Malaisse, W. J. (1999) *Metab. Clin. Exp.* **48,** 779–785
28. Demontis, S., Rigo, C., Piccinin, S., Mizzau, M., Sonego, M., Fabris, M., Brancolini, C., and Maestro, R. (2006) *Cell Death Differ.* **13,** 335–345
29. Li, H., Zhu, H., Xu, C. J., and Yuan, J. (1998) *Cell* **94,** 491–501
30. Gerner, C., Frohwein, U., Gotzmann, J., Bayer, E., Gelbmann, D., Bursch, W., and Schulte-Hermann, R. (2000) *J. Biol. Chem.* **275,** 39018–39026
31. Van Damme, P., Martens, L., Van Damme, J., Hugelier, K., Staes, A., Vandekerckhove, J., and Gevaert, K. (2005) *Nat. Methods* **2,** 771–777
32. Colell, A., Ricci, J. E., Tait, S., Milasta, S., Maurer, U., Bouchier-Hayes, L., Fitzgerald, P., Guio-Carrion, A., Waterhouse, N. J., Li, C. W., Mari, B., Barbry, P., Newmeyer, D. D., Beere, H. M., and Green, D. R. (2007) *Cell* **129,** 983–997
33. van de Water, B., Tijdens, I. B., Verbrugge, A., Huigsloot, M., Dihal, A. A., Stevens, J. L., Jaken, S., and Mulder, G. J. (2000) *J. Biol. Chem.* **275,** 25805–25813
34. Browne, K. A., Johnstone, R. W., Jans, D. A., and Trapani, J. A. (2000) *J. Biol. Chem.* **275,** 39262–39266
35. Kothakota, S., Azuma, T., Reinhard, C., Klippel, A., Tang, J., Chu, K., McGarry, T. J., Kirschner, M. W., Koths, K., Kwiatkowski, D. J., and Williams, L. T. (1997) *Science* **278,** 294–298
36. Byun, Y., Chen, F., Chang, R., Trivedi, M., Green, K. J., and Cryns, V. L. (2001) *Cell Death Differ.* **8,** 443–450
37. Mashima, T., Naito, M., Noguchi, K., Miller, D. K., Nicholson, D. W., and Tsuruo, T. (1997) *Oncogene* **14,** 1007–1012
38. Prasad, S., Soldatenkov, V. A., Srinivasarao, G., and Dritschilo, A. (1998) *Int. J. Oncol.* **13,** 757–764
39. Brockstedt, E., Rickers, A., Kostka, S., Laubersheimer, A., Dorken, B., Wittmann-Liebold, B., Bommert, K., and Otto, A. (1998) *J. Biol. Chem.* **273,** 28057–28064
40. Thiede, B., Dimmler, C., Siejak, F., and Rudel, T. (2001) *J. Biol. Chem.* **276,** 26044–26050

The Caspase-1 Digestome Identifies the Glycolysis Pathway as a Target during Infection and Septic Shock

Wei Shao, Garabet Yeretssian, Karine Doiron, Sabah N. Hussain and Maya Saleh

J. Biol. Chem. 2007, 282:36321-36329.
doi: 10.1074/jbc.M708182200 originally published online October 24, 2007
